Small bodies of the solar system

Lecture by Klaus Jockers, Göttingen, winter term 2004/2005

Comets2

Comet-solar wind interaction: a phenomenological view

Motion of cometary plasma tails in the solar wind

Plasma tails are formed by cometary ions dragged away from the comet by the solar wind.

Comet tails can be very long, up to 1 AU!

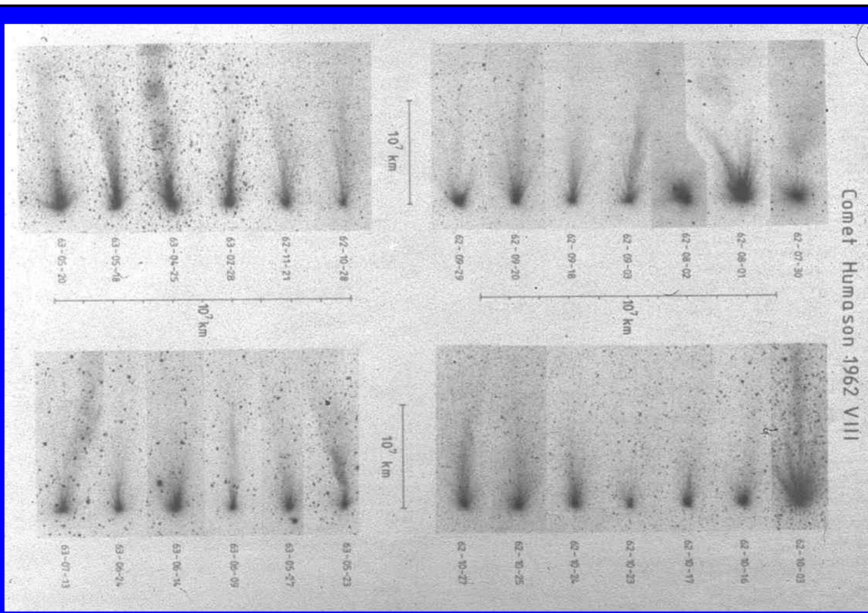

Observations of the CO+ tail of comet Humason 1962 VIII (courtesy EH Geyer, Bonn). Note plasma tail direction changes, tail kinks and clouds. We look at the comet with a small phase angle which exaggerates lateral displacements.

Solar wind stream interface

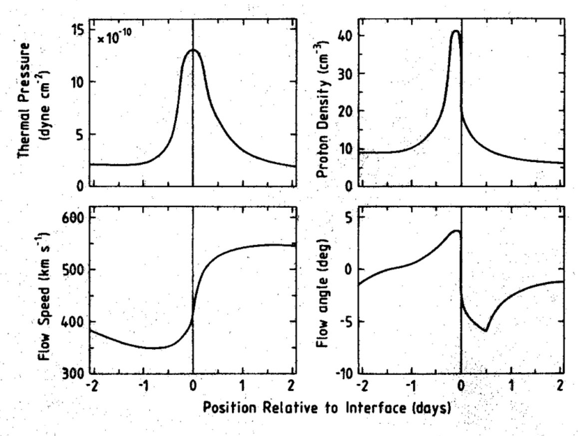

FIGURE 17. — Pressure, proton number density, flow speed and flow angle of a typical solar wind stream interface (after Gosling *et al.*, 1978).

Sometimes, but not always, stream interfaces are associated with magnetic field reversals

The most trivial effect is a tail direction change caused by a solar wind direction change.
A: “old” tail, unaffected by change.
B: intermediate tail segment, emitted before the change and now affected by the change.
C: “new” tail, unaffected by the change.
Along section B the solar wind flows across the tail and a Rayleigh-Taylor type instability developes.

For this and the following slides see:
Jockers K., Astron. Astrophys. Suppl. Ser. 62, 791-838.
Jockers K. in Johnstone ed. Cometary Plasma Processes, 139-152.

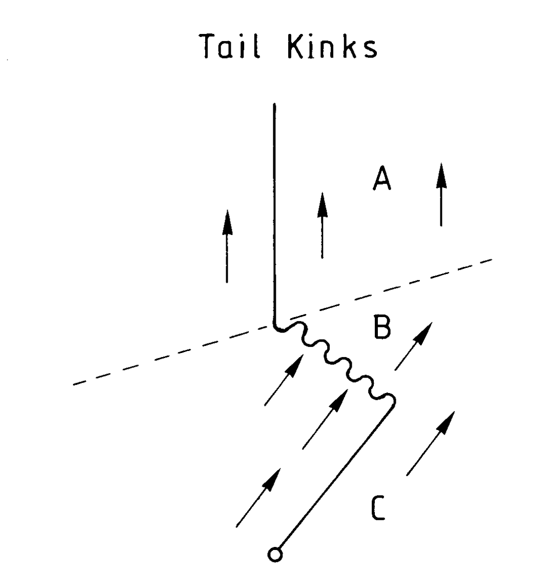

Fig. 8. Pair of kinks and associated Rayleigh-Taylor instability in a cometary tail (see text), caused by a solar wind direction change.

Comet Kohoutek: The interaction region of the preceding slide with the velocity change in the line of sight.
b: Sketch of a.
c: b as the tail may look like from a direction turned around by 90^0 with respect to b.

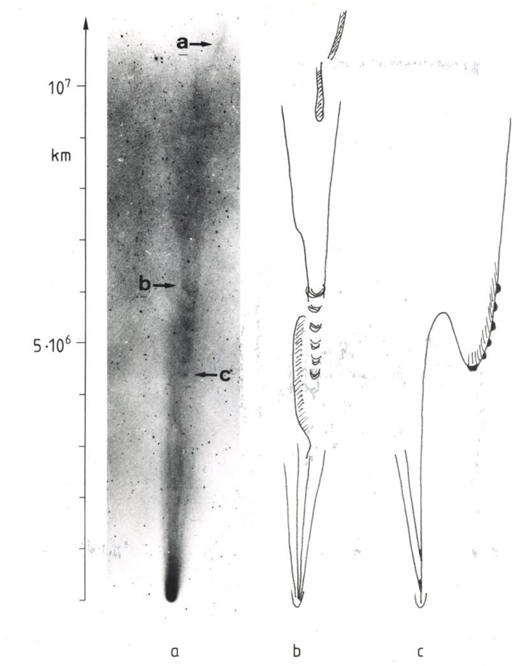

Comet Bennett: Velocity vectors have been derived from a series of observations (left side). Where the vectors are not parallel to the tail axis Rayleigh-Taylor waves develop (arrows in the photograph).

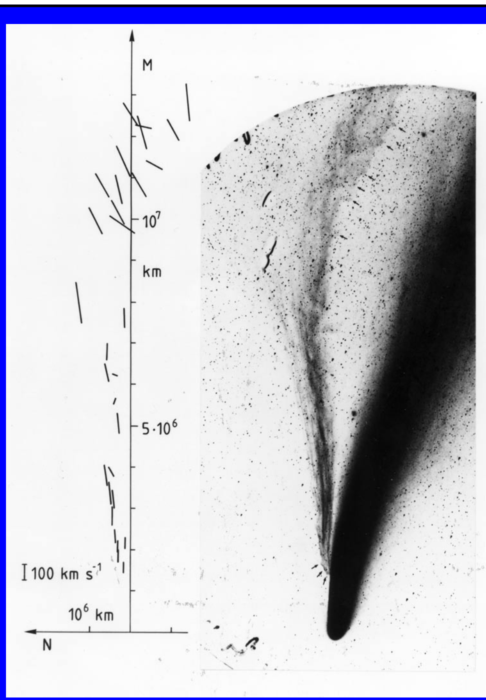

Tail rays, one-sided and two-sided

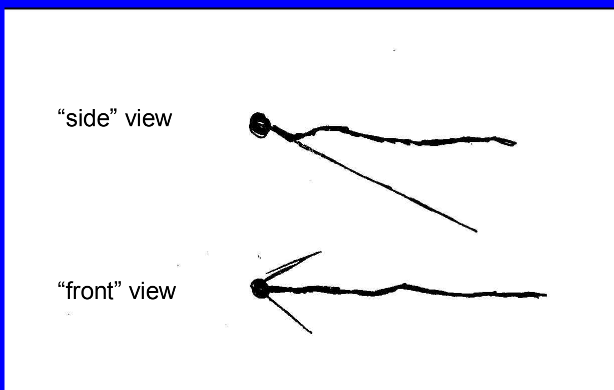

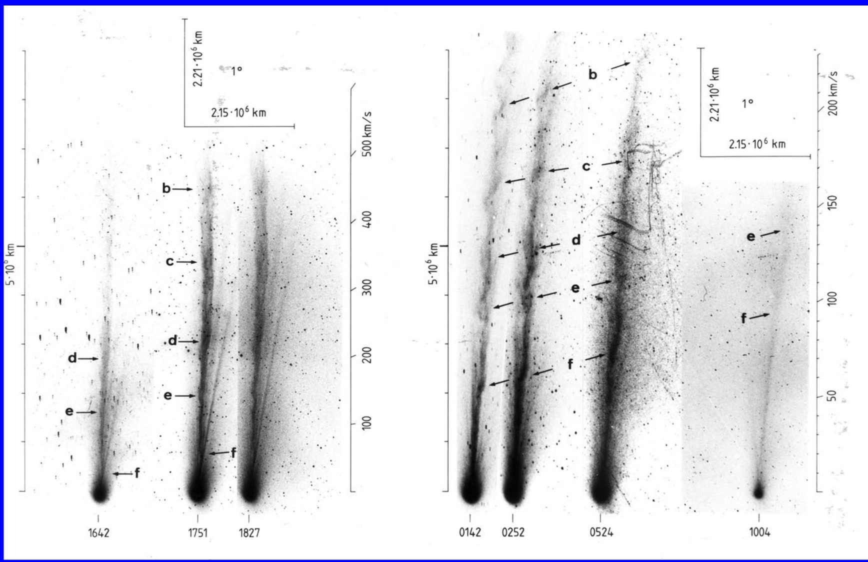

One-sided tail rays: After a few hours (the numbers under the images are hours UT) the mail tail turns into the direction where rays have appeared. Note again the Rayleigh-Taylor waves. The stronger ones are marked with letters.

A similar event like on the previous slide: In the left image a tail ray appears on the left side of the main tail. Arrows mark Rayleigh-Taylor structures.

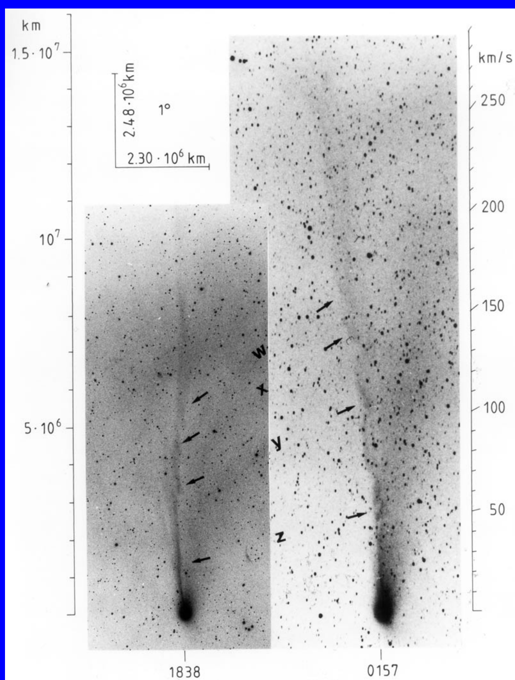

Clouds in the tail of comet Humason. Some may call this a tail disconnection event. Clouds are frequently associated with tail ray phenomena, but I doubt that the reason for this is reconnection as was put forward in the literature. Note that the tail rays in these two images, in particular in the left one, are symmetric, in contrast to the one-sided rays we have seen before. The symmetric rays may be inclined with respect to the projection plane. To an observer located in the projection plane the rays may look as one-sided.

Tail disconnection events caused by solar wind compression and direction change or by magnetic field reversal?

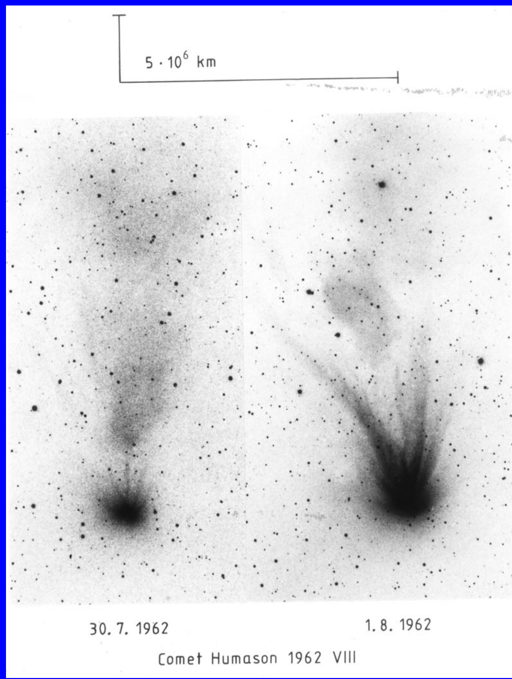

Another case of symmetric tail rays is observed here in comet Kobayashi-Berger-Milon 1975 IX = C/1975 N1. There is no clear association with a cloud as in the previous slide.

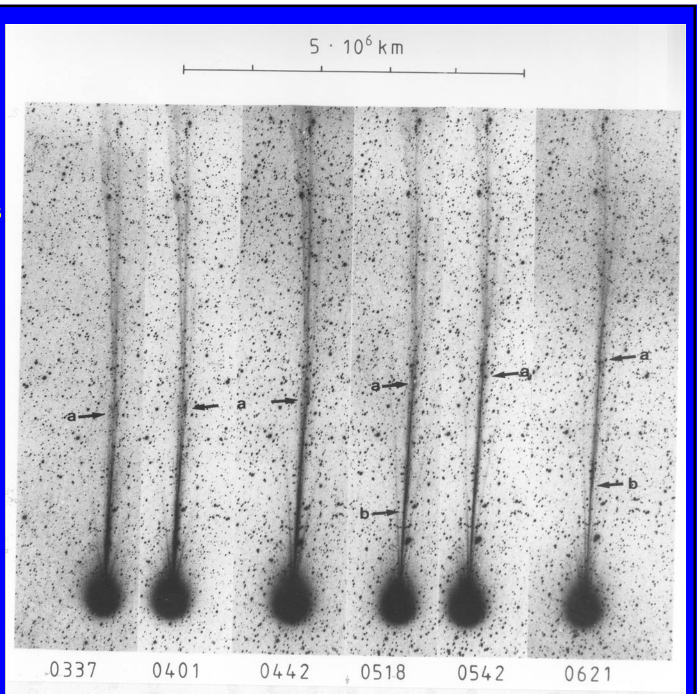

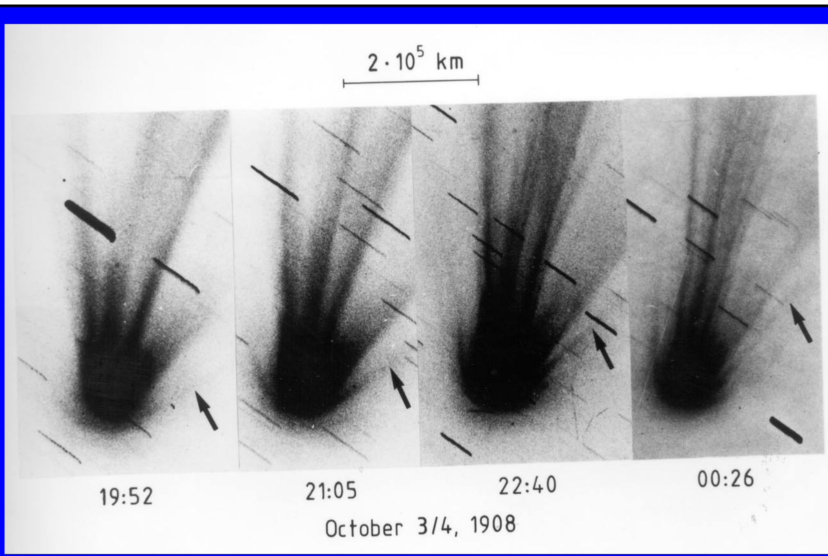

In comet C/1908 R1 (Morehouse) (=1908 III), another CO-rich comet, tail rays are paired, actually (which is difficult to see here) ray pairs connect in front of the cometary head to enveloppes. They have been described and measured by Eddington (1910, MNRAS 70, 442)

Steady Comet – Solar Wind Interaction

Besides of particle codes, MHD models also provide inside into the comet-solar wind interaction . The following literature may be of interest:
Alan D. Johnstone ed. "Cometary plasma processes", AGU Geophysical monograph 61, 1991.
Wegmann R., Astron. Astrophys. 294, 601-614, 1995.
Wegmann R., Jockers K., Bonev T., Planet. Sp. Sci. 47, 745-763, 1999.
The two last papers deal with the "similarity theorem":
An important length scale in the problem of comet-solar wind interaction is:

$$R_I = \frac{\sigma m_C G}{4\pi w \rho_\odot u_\odot}$$

σ is average rate of ionization, m_C average mass of a cometary ion, *G* production rate of neutral atoms, *w* is the mean outflow speed of neutrals ≈ 1 km s^{-1}, ρ_o and u_o are solar wind density and flow speed.
This means that the size of the interaction region approximately scales with the production rate *G* of the comet. For instance the standoff distance of the bow shock is given by (γ2 – 1) RI, where γ is the specific heat ratio.

In what follows I present own results on observations of cometary plasma tails relevant to the problem of comet-solar wind interaction.

Magneto-hydrodynamic equations of comet-solar wind interaction

Wegmann R., Astron. Astrophys. 294, 601-614, 1995.

$$\frac{\partial \rho}{\partial t} + \operatorname{div} \rho \boldsymbol{u} = \dot{\rho},$$

Mass source (the only source that needs to be considered)

$$\frac{\partial n}{\partial t} + \operatorname{div} n\boldsymbol{u} = \dot{n},$$

Number density source

$$\frac{\partial \rho \boldsymbol{u}}{\partial t} + \operatorname{div} \rho \boldsymbol{u} \cdot \boldsymbol{u} + \operatorname{grad} p - \frac{1}{4\pi}(\operatorname{curl} \boldsymbol{B}) \times \boldsymbol{B} = \dot{\boldsymbol{q}},$$

$$\frac{\partial}{\partial t}\left(\frac{\rho u^2}{2} + \frac{p}{\gamma - 1} + \frac{B^2}{8\pi}\right) + \operatorname{div}\left(\frac{\rho u^2}{2} + \frac{\gamma p}{\gamma - 1} + \frac{B^2}{4\pi}\right)\boldsymbol{u} - \frac{1}{4\pi}\operatorname{div}(\boldsymbol{u}, \boldsymbol{B})\boldsymbol{B} = \dot{e},$$

$$\frac{\partial \boldsymbol{B}}{\partial t} - \operatorname{curl}(\boldsymbol{u} \times \boldsymbol{B}) = 0.$$

$$N_n = \frac{G}{4\pi w R^2} \exp\left(-\frac{\sigma R}{w}\right).$$

$$\dot{n} = \sigma N_n, \qquad \dot{\rho} = \sigma N_n m_C + \sigma_{ce} N_n (m_C - m_I),$$

$$\dot{\boldsymbol{q}} = -\sigma_{ce} N_n m_I \boldsymbol{u}, \qquad \dot{e} = -\sigma_{ce} N_n \left(\frac{m_I u^2}{2} + \frac{p}{(\gamma - 1)n}\right)$$

Discontinuity surfaces

For the solar wind a comet is an extended ion source. Ionization time scales are in the range of 10^6 to 10^7 sec, i.e. of a few weeks to a few months.

K. Jockers, in ACM III, Lagerkvist et al. eds., p. 353-361

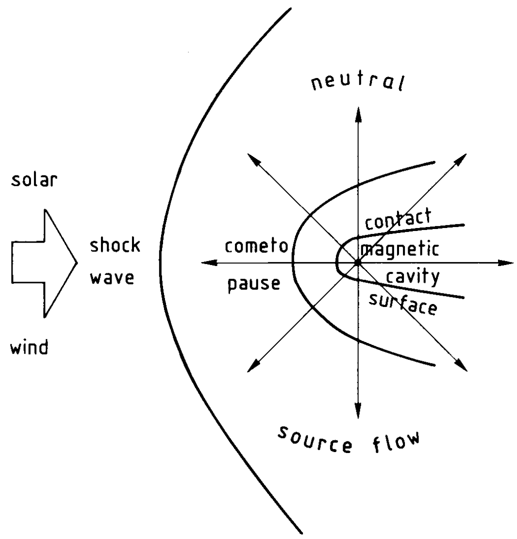

Fig. 1 Boundaries in the comet-solar wind interaction (for the scales see Table 1).

Table 1

Spacecraft Encounters with Comets

Giacobini–Zinner	ICE	
time of closest encounter	1985–09–11	11:02 UT
helioc. distance	1.03 au	
geoc. distance	0.47 au	
ICE closest approach	7800 km	tailward
magnetotail diameter	9600 km	
current sheet diameter	$\sim$ 2000 km	

K. Jockers, in ACM III, Lagerkvist et al. eds., p. 353-361

Spacecraft encounters with comets, continued

Halley	Vega 1	Vega 2	Giotto	
date of closest encounter	1986–03–06	1986–03–09	1986–03–14	
time of closest encounter	7:20 UT	7:20 UT	0:03 UT	
heliocentric distance (au)	0.79	0.83	0.90	
geocentric distance (au)	1.15	1.08	0.96	
closest approach km	8890	8030	605	sunward
diameter magnetic cavity	9000 km			
diameter cometopause	3×10^5 km			
shock wave stand–off distance	10^6 km			

Production rate of comet Halley ≈ 10^{30} water molecules s^{-1}.

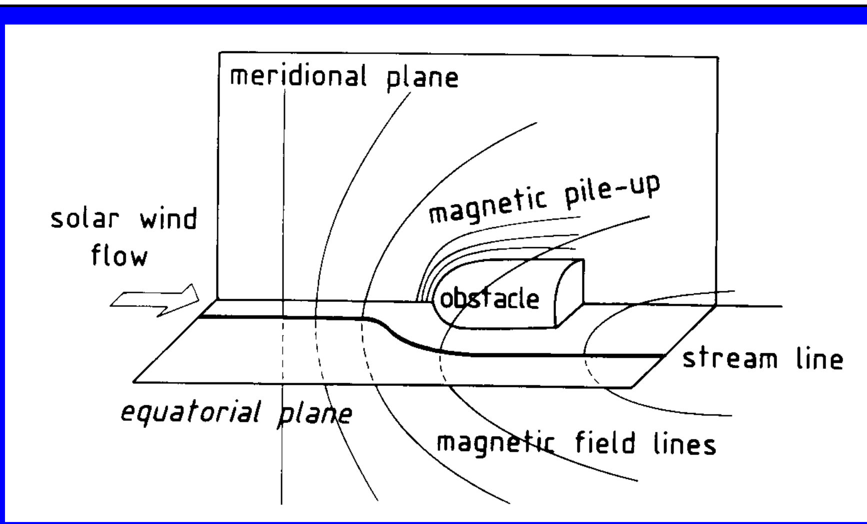

The interaction of the solar wind with the comet is truly three-dimensional, despite of the high plasma beta. On the stagnation flow line the magnetic pressure balances the solar wind momentum. This was confirmed by the space probe fly-bys. The flow speed is higher in the "equatorial plane" (also called "magnetic equator"). Under stationary conditions the plasma tail is flat like a beaver tail and extended in the equatorial plane.

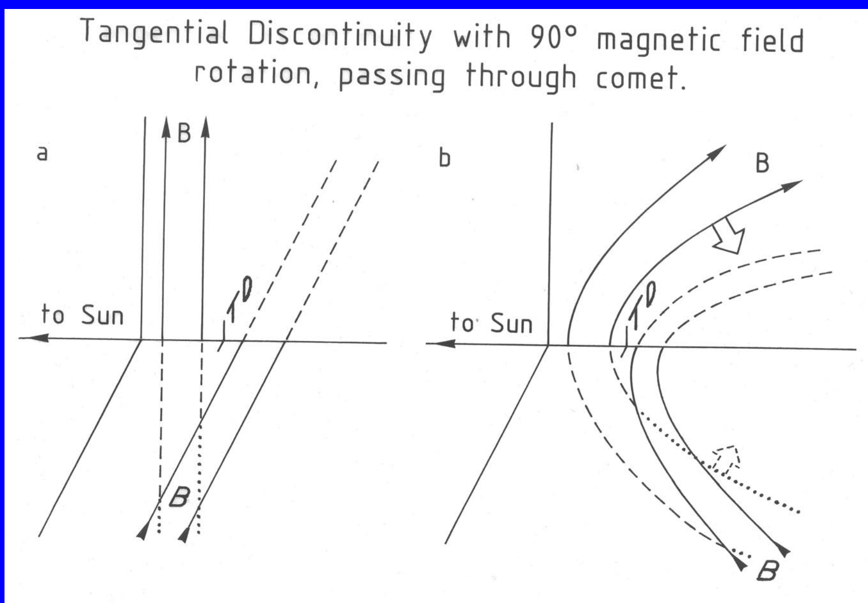

In the previous slide we have seen what happens if a tangential discontinuity with a magnetic field direction change passes through a comet. The plane of the beaver tail must turn around, in this case by 90^0. Two different magnetic layers are put on top of each other and, if there are more such discontinuities, the tail gets an onion skin structure. One theory put forward by HU Schmidt and Wegmann (in LL Wilkening ed., Comets, pp. 538-560, Tucson 1983, R. Wegmann, ASTRON ASTROPHYS 358 (2): 759-775, 2000) tries to explain tail rays that way.

As the cometary plasma is created by ionization of the neutral cloud (gas coma) surrounding the nucleus it is of interest to observe the cometary plasma close to the nucleus. This can be done with Fabry-Perots working as tunable filters with a bandwidth of several Å only. The following slides present such work (Bonev and Jockers, H_2O^+ ions in the inner plasma tail of Comet Austin 1990 V, Icarus 107, 335-357, 1994, Bonev's ph. d. thesis). In the following images the dust continuum and coma emissions are suppressed. We first present some data which show how the tail rays grow from a plasma coma and then present the one-dimensional mass balance (integrated in planes perpendicular to the tail axis).

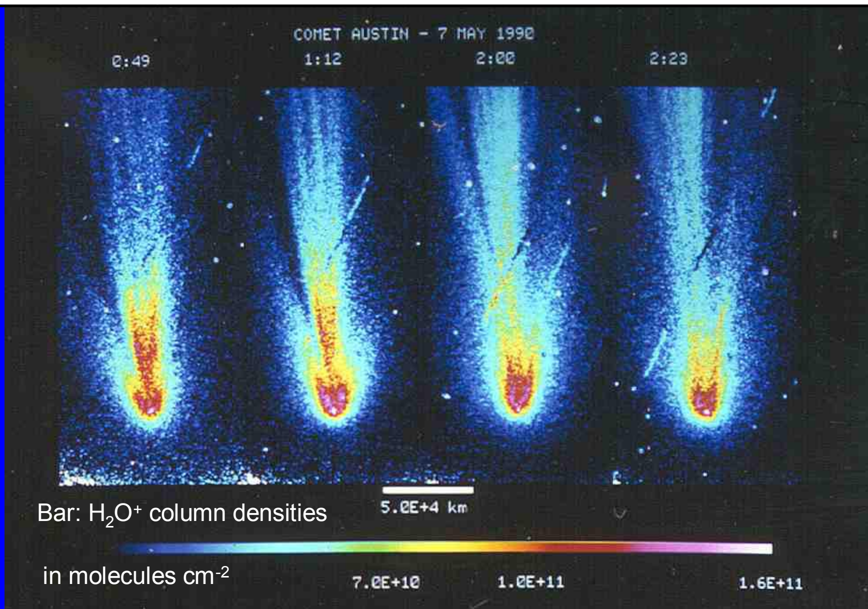

Tail rays grow and central tail dies out.

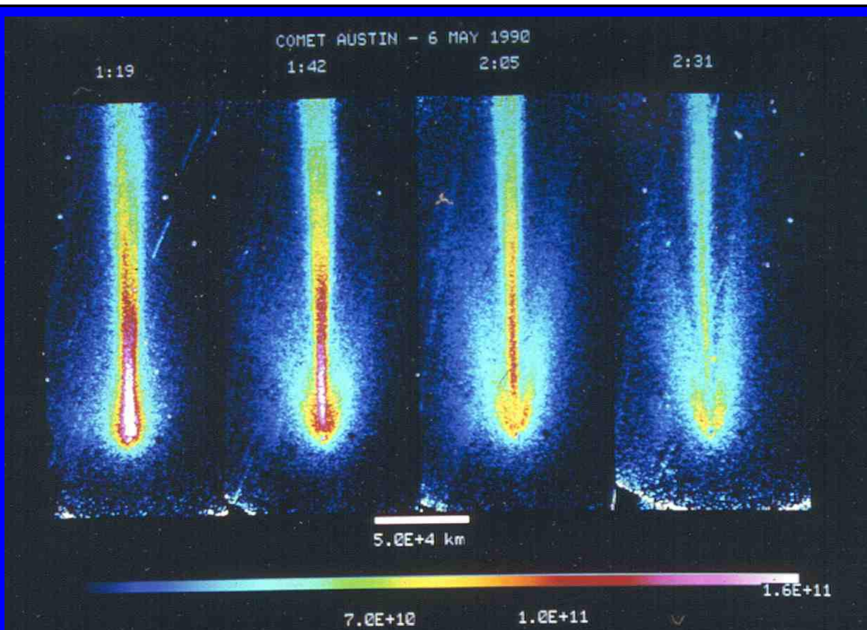

These images may be explained by the effect of magnetic field tangential discontinuity. In the first two images we are very close to the magnetic equator, in the last two images the new magnetic equator is in the projection plane.

Isocontours and black and white rendered versions of the images of May 4. The enhanced contour is 10^{11} molecules cm^{-2}.

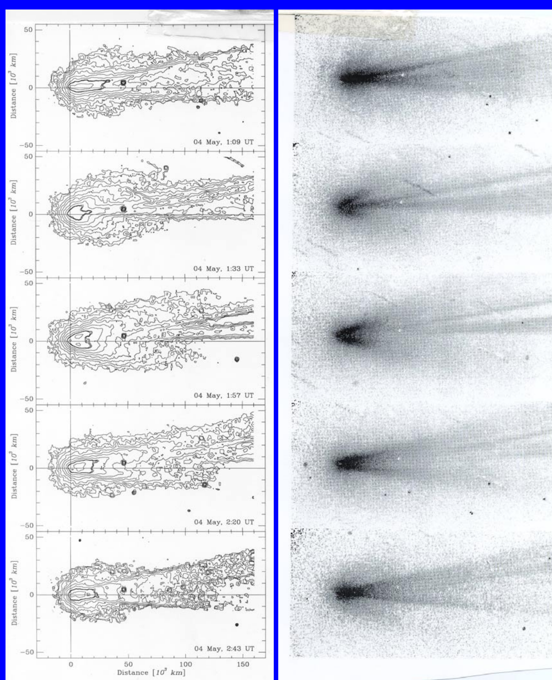

Isocontours and black and white rendered versions of the images of May 6. The enhanced contour is 1011 molecules cm-2.

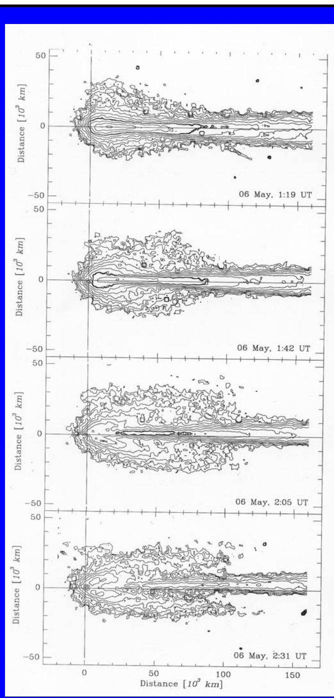

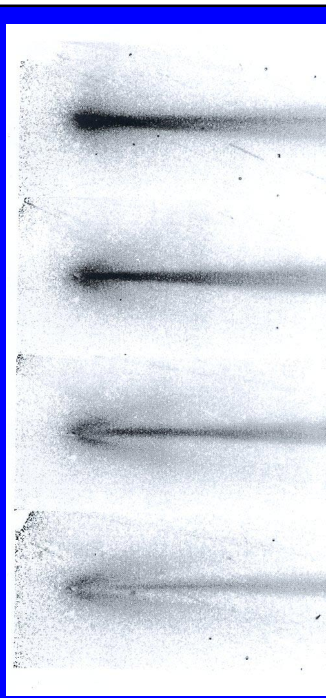

Ions per tail length, i. e. integrated over planes perpendicular to the tail axis (the phase angle is close to 90^0)

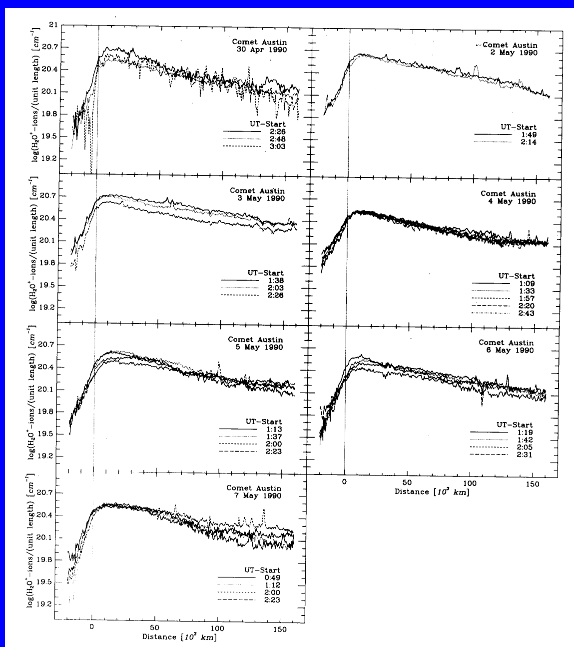

FIG. 12. Number of ions per unit tail length. The maxima are shifted tailward.

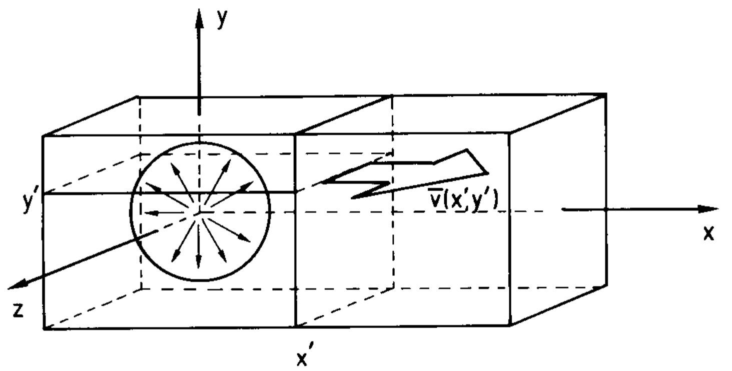

FIG. 11. The spherically expanding neutral source and the idealized plasma flow.

The box of the integrations. z points towards the observer. The aim is to provide a mass balance across the tail, i. e. integrated over y and z.

$$\nabla \cdot (n\mathbf{v}) = A, \quad \text{Ion source} \tag{8}$$

σ_i is the ionization cross-section and σ_d the destruction cross-section of the neutrals.

$$A = \sigma_i N_n = \frac{\sigma_i G}{4\pi v_e R^2} \exp\left(-\frac{\sigma_d R}{v_e}\right). \tag{9}$$

From (8)
With Gauss theorem:

$$\int\int n(x, y, z)\, \mathbf{v}(x, y, z)\, d\mathbf{S} = \int\int\int A\, dV, \tag{10}$$

Use the box:

$$\int_{-\infty}^{\infty} dy \int_{-\infty}^{\infty} dz\, n(x', y, z)\, v_x(x', y, z) = \int_{-\infty}^{x'} dx \int_{-\infty}^{\infty} dy \int_{-\infty}^{\infty} dz\, A. \tag{11}$$

Define average speed:

$$\bar{v}_x(x') = \frac{\int_{-\infty}^{\infty} dy \int_{-\infty}^{\infty} dz\, n(x', y, z)\, v_x(x', y, z)}{\int_{-\infty}^{\infty} dy \int_{-\infty}^{\infty} dz\, n(x', y, z)}, \tag{12}$$

From (11):

$$\bar{v}_x(x') \int_{-\infty}^{\infty} dy \int_{-\infty}^{\infty} dz\, n(x', y, z) = \int_{-\infty}^{x'} dx \int_{-\infty}^{\infty} dy \int_{-\infty}^{\infty} dz\, A. \tag{13}$$

Ions per tail length:

$$\int_{-\infty}^{\infty} dy \int_{-\infty}^{\infty} dz\, n(x', y, z) = \int_{-\infty}^{\infty} dy\, N(x', y). \tag{14}$$

The integral can be solved with special functions:

$$\int_{-\infty}^{x'} dx \int_{-\infty}^{\infty} dy \int_{-\infty}^{\infty} dz\, A$$

Ei is the exponential integral function.

$$= \frac{\sigma_i G}{2 v_e \beta} \begin{cases} \exp(\beta x') - \beta x' \mathrm{Ei}(\beta x') & x' \leq 0 \\ 2 - \exp(-\beta x') + \beta x' \mathrm{Ei}(-\beta x') & x' > 0. \end{cases} \tag{15}$$

Finally, x' →∞ for the total source rate:

$$\int_{-\infty}^{\infty} dx \int_{-\infty}^{\infty} dy \int_{-\infty}^{\infty} dz\, A = \frac{\sigma_i G}{\sigma_d}. \tag{16}$$

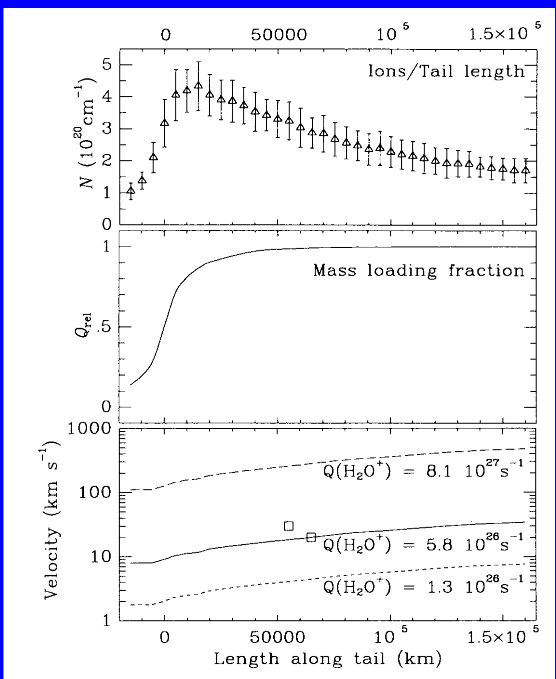

Top: Mean number of water ions per tail length and standard deviation (error bars).

Middle: Fraction of the H2O+ source which has already been ionized at a given distance (abscissa) from the nucleus (eq. (15)).

Bottom: Mean velocity calculated from the observed number of ions per tail length and the source integral. Long dash: Theoretical curve. Full line: Curve fitted to velocity measurement. Short dash: Water production rate from Schultz et al. (Icarus 104, 185-196, 1993).

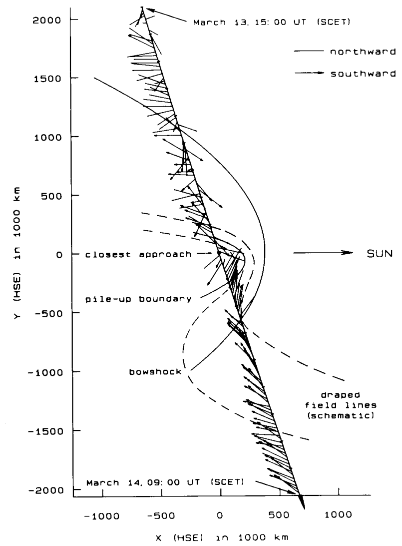

Fig. 1. Four-minute averaged magnetic field unit vectors, decimated by 2 and projected onto the *X–Y* plane of the Halley Solar Ecliptic System (HSE) from 15 UT on March 13 to 9 UT on March 14. The length of the vectors is proportional to the cosine of the elevation angle with respect to the *X–Y* plane. Ticmarcs on the trajectory are 1 h apart. The bowshock and the pile-up boundary are indicated together with two schematically drawn draped field lines

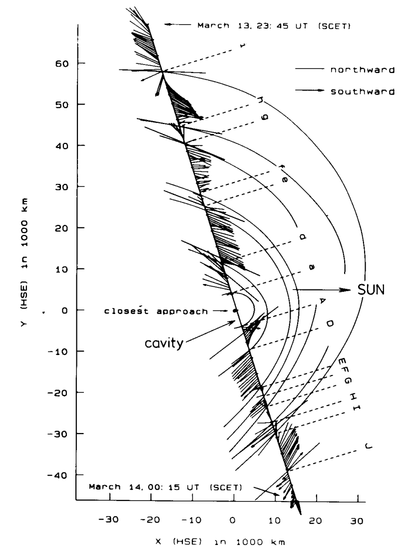

Fig. 3. Section of Fig. 2 from 23:45 UT March 13 to 00:15 UT March 14. The 4 s averages are decimated by 2. The magnetic layers with different polarity are sketched here

Onion shell-like magnetic surfaces observed in comet Halley during Giotto flyby.